Journal of Computational Science and Technology

Vol. 3, No. 1, 2009

Variations of Stress Intensity Factors of a Planar Interfacial Crack Subjected to Mixed Mode Loading*

Chunhui XU**, Nao-Aki NODA*** and Yasushi TAKASE****
**College of Science, China Agricultural University, Beijing 100083, P.R.CHINA
E-mail:xuchunhui_cau@163.com
***Department of Mechanical Engineering, Kyushu Institute of Technology
Sensui-Cho 1-1 Tobata-Ku, Kitakyushu-Shi, Fukuoka, Japan
E-mail: noda@mech.kyutech.ac.jp
****Department of mechanical Engineering, Kyushu Institute of Technology
Sensui-Cho 1-1 Tobata-Ku, Kitakyushu-Shi, Fukuoka, Japan
E-mail: takase@mech.kyutech.ac.jp

Abstract
In this paper, a mixed-mode interfacial crack in three dimensional bimaterials is analyzed by singular integral equations on the basis of the body force method. In the numerical analysis, unknown body force densities are approximated by the products of the fundamental density functions and power series, where the fundamental density functions are chosen to express a two-dimensional interface crack exactly. The results show that the present method yields smooth variations of mixed mode stress intensity factor along the crack front accurately. The effect of crack shape on the stress intensity factor for 3D interface cracks is also discussed on the basis of present solution. Then, it is found that the stress intensity factors K_{II} and K_{III} are always insensitive to the varying ratio of shear modulus, and determined by Poisson's ratio alone. Distributions of stress intensity factor are indicated in tables and figures with varying the rectangular shape and Poisson's ratio.

Key words: Stress Intensity Factor, Body Force Method, Interface Crack, Composite Material, Singular Integral Equation

1. Introduction

Recently, adhesive joints and composite materials are widely used for lightweight and functional structures; and therefore, to evaluate their strength has become an important issue especially from the viewpoint of interfacial destruction, which controls the failure of those structures. For interfacial crack problem, exact analyses are difficult because of the peculiar behavior of oscillation stress singularity at the interface crack tip. Regarding three-dimensional problems, penny-shaped crack [1]-[5] and elliptical interfacial crack[6] were treated with the problem in a finite body [7]; however, most numerical calculations were preformed only under specific combination of materials combinations. Closed form solutions of stress intensity factors (SIFs) are available only for a penny-shaped [7] and external deep interfacial crack [8] under arbitrary combinations of materials.

In our previous papers [9], an axi-symmetric ring-shaped interfacial crack under tension and torsion in dissimilar materialwere analyzed on the idea of the body force method coupled with singular integral equation formulation. In the numerical solutions, the unknown

*Received 19 Dec., 2008 (No. T1-06-1196)
Japanese Original : Trans. Jpn. Soc. Mech. Eng., Vol.73, No.731, A (2007), pp.768-774 (Received 11 Dec., 2006)
[DOI: 10.1299/jcst.3.232]

functions were approximated by the products of the fundamental density functions and polynomials [9] - [11].

In the preceding papers [12], [13], a rectangular crack under tension was analyzed and smooth distributions of SIFs were obtained. Although the problem of an interface crack in a dissimilar material is expressed as a system of singular integral equations by Chen-Noda-Tang [14], it is difficult to solve the equations precisely considering the overlap of crack opening displacement and stress oscillation singularity, which are peculiar to interfacial cracks.

In this paper, accurate numerical solutions are discussed for interface crack under shear loading considering singular behavior exactly; then, the stress intensity factors of a rectangular interfacial crack are discussed. The unknown body force densities will be approximated by using the fundamental density functions, which express singular stress fields exactly. It should be noted that the present method has a specific advantage that the stress intensity factors are directly determined from the solutions of unknown densities.

2. Singular intergro-differential equations for 3D biomaterial interfacial crack problems

Consider two dissimilar elastic half-spaces bonded together along the $x-y$ plane under shear loading $\tau_{yz}^{\infty}=1$ ($\sigma_z^{\infty}=0, \tau_{zx}^{\infty}=0$) at infinity as shown in Fig.1, which include a rectangular crack on the interfacial whose length and width are 2a and 2b respectively. The notations μ_1, μ_2 denote shear modulus, and ν_1, ν_2 Poisson ratios for upper and lower spaces. The hypersingular intergro-differential equations (1a)-(1e) for this interfacial crack problem, which were derived by Chen-Noda-Tang [14], are expressed in the following equations.

$$\mu_1(\Lambda_2-\Lambda_1)\frac{\partial \Delta u_z(x,y)}{\partial x}+\mu_1\frac{(2\Lambda-\Lambda_1-\Lambda_2)}{2\pi}\oint_s \frac{1}{r^3}\Delta u_x(\xi,\eta)dS(\xi,\eta)$$
$$+3\mu_1\frac{(\Lambda_1+\Lambda_2-\Lambda)}{2\pi}\left\{\oint_s \frac{(x-\xi)^2}{r^5}\Delta u_x(\xi,\eta)dS(\xi,\eta)+\oint_s \frac{(x-\xi)(y-\eta)}{r^5}\Delta u_y(\xi,\eta)dS(\xi,\eta)\right\}=-p_x(x,y) \quad (1a)$$

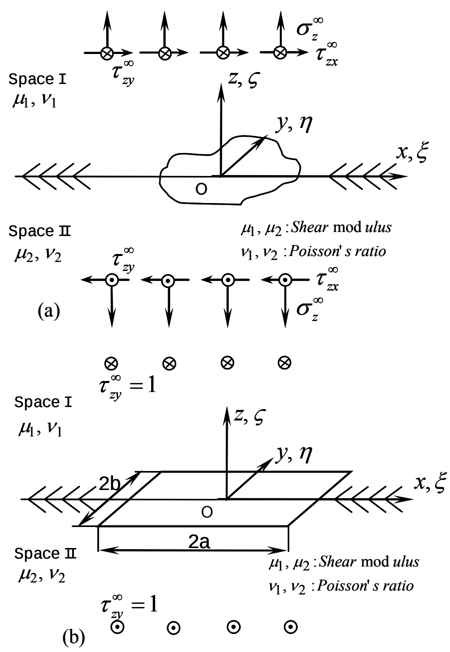

Fig.1 Problem configuration

$$\mu_1\left(\Lambda_2-\Lambda_1\right)\frac{\partial \Delta u_z\left(x,y\right)}{\partial y}+\mu_1\frac{\left(2\Lambda-\Lambda_1-\Lambda_2\right)}{2\pi}\fint_s \frac{1}{r^3}\Delta u_y(\xi,\eta)dS(\xi,\eta)$$
$$+3\mu_1\frac{\left(\Lambda_1+\Lambda_2-\Lambda\right)}{2\pi}\left\{\fint_s \frac{(x-\xi)(y-\eta)}{r^5}\Delta u_x(\xi,\eta)dS(\xi,\eta)+\fint_s \frac{(y-\eta)^2}{r^5}\Delta u_y(\xi,\eta)dS(\xi,\eta)\right\}=-p_y(x,y) \tag{1b}$$

$$\mu_1\left(\Lambda_1-\Lambda_2\right)\left(\frac{\partial \Delta u_x\left(x,y\right)}{\partial x}+\frac{\partial \Delta u_y\left(x,y\right)}{\partial y}\right)+\mu_1\frac{\left(\Lambda_1+\Lambda_2\right)}{2\pi}\fint_s \frac{1}{r^3}\Delta u_z(\xi,\eta)dS(\xi,\eta)=-p_z\left(x,y\right) \tag{1c}$$

$$\left(x,y\right)\in S,$$

$$\Lambda=\frac{\mu_2}{\mu_1+\mu_2},\quad \Lambda_1=\frac{\mu_2}{\mu_1+\kappa_1\mu_2},\quad \Lambda_2=\frac{\mu_2}{\mu_2+\kappa_2\mu_1},$$
$$\kappa_1=3-4\nu_1,\quad \kappa_2=3-4\nu_2,\quad r^2=\left(x-\xi\right)^2+\left(y-\eta\right)^2 \tag{1d}$$

$$\Delta u_i\left(x,y\right)=u_i(x,y,0^+)-u_i(x,y,0^-),(i=x,y,z). \tag{1e}$$

Here, $\Delta u_i(x,y)$ means the crack opening displacement on the interface in the i direction, and the integral $\fint_s$ should be interpreted in a sense of finite part integral.

3. Numerical solutions

In the numerical solutions of the conventional body force method, the unknown body force densities are approximated by using step functions. Since unknown densities are continuous functions, the final results are obtained by extrapolation; and therefore, smooth distributions of stress intensity factors are difficult to be obtained. In this paper following expressions are applied to approximate the unknowns as continuous functions.

$$\Delta u_i\left(\xi,\eta\right)=w_i(\xi,\eta)F_i(\xi,\eta),\ \ i=x,y,z \tag{2}$$

$$\left.\begin{aligned}
w_x(\xi,\eta)&=\sum_{l=1}^{2}\frac{1+\kappa_l}{4\mu_l\cosh\pi\varepsilon}\sqrt{a^2-\xi^2}\sqrt{b^2-\eta^2}\times\sin\left(\varepsilon\ln\left(\frac{a-\xi}{a+\xi}\right)\right)\\
w_y(\xi,\eta)&=\sum_{l=1}^{2}\frac{1+\kappa_l}{4\mu_l\cosh\pi\varepsilon}\sqrt{a^2-\xi^2}\sqrt{b^2-\eta^2}\times\sin\left(\varepsilon\ln\left(\frac{b-\eta}{b+\eta}\right)\right)\\
w_z(\xi,\eta)&=\sum_{l=1}^{2}\frac{1+\kappa_l}{4\mu_l\cosh\pi\varepsilon}\sqrt{a^2-\xi^2}\sqrt{b^2-\eta^2}\times\cos\left(\varepsilon\ln\left(\frac{a-\xi}{a+\xi}\right)\right)\cos\left(\varepsilon\ln\left(\frac{b-\eta}{b+\eta}\right)\right)
\end{aligned}\right\} \tag{3}$$

Here $w_x(\xi,\eta), w_y(\xi,\eta), w_z(\xi,\eta)$ are called fundamental density functions, which express singular behavior along the crack front exactly when the rectangular interface crack is subjected to shear τ_{yz}^{∞}. In real calculations we may put $\tau_{yz}^{\infty}=1$. The bimaterial constant ε is defined as follows.

$$\varepsilon=\frac{1}{2\pi}\ln\left(\frac{\mu_2\kappa_1+\mu_1}{\mu_1\kappa_2+\mu_2}\right)$$

Weight functions $F_x(\xi,\eta), F_y(\xi,\eta), F_z(\xi,\eta)$ are approximated by polynomials as continuous functions.

$$\left.\begin{aligned}
&F_x(\xi,\eta)=\alpha_0+\alpha_1\eta+\cdots+\alpha_{n-1}\eta^{(n-1)}+\alpha_n\eta^n+\alpha_{n+1}\xi+\alpha_{n+2}\xi\eta+\cdots+\alpha_{2n}\xi\eta^n+\cdots\\
&+\alpha_{l-n-1}\xi^m+\alpha_{l-n}\xi^m\eta+\cdots+\alpha_{l-1}\xi^m\eta^n=\sum_{i=0}^{l-1}\alpha_i G_i(\xi,\eta)\\
&F_y(\xi,\eta)=\beta_0+\beta_1\eta+\cdots+\beta_{n-1}\eta^{(n-1)}+\beta_n\eta^n+\beta_{n+1}\xi+\beta_{n+2}\xi\eta+\cdots+\beta_{2n}\xi\eta^n+\cdots\\
&+\beta_{l-n-1}\xi^m+\beta_{l-n}\xi^m\eta+\cdots+\beta_{l-1}\xi^m\eta^n=\sum_{i=0}^{l-1}\beta_i G_i(\xi,\eta)\\
&F_z(\xi,\eta)=\gamma_0+\gamma_1\eta+\cdots+\gamma_{n-1}\eta^{(n-1)}+\gamma_n\eta^n+\gamma_{n+1}\xi+\gamma_{n+2}\xi\eta+\cdots+\gamma_{2n}\xi\eta^n+\cdots\\
&+\gamma_{l-n-1}\xi^m+\gamma_{l-n}\xi^m\eta+\cdots+\gamma_{l-1}\xi^m\eta^n=\sum_{i=0}^{l-1}\gamma_i G_i(\xi,\eta)
\end{aligned}\right\} \tag{4}$$

$l=(n+1)(m+1), G_0(\xi,\eta)=1,\ \ G_1(\xi,\eta)=\eta,\ \ \cdots, G_{n+1}(\xi,\eta)=\xi,\ \ \cdots, G_{l-1}(\xi,\eta)=\xi^m\eta^n.$

Using the approximation method mentioned above, we obtain the following system of linear equations for the determination of the coefficients $\alpha_i,\beta_i,\gamma_i$. The unknown coefficients $\alpha_i,\beta_i,\gamma_i$, whose number is 3l, are then determined from (5) by selecting a set of collocation points to minimize the residual stresses.

$$\left.\begin{aligned}
&\sum_{i=0}^{l-1}\alpha_i(f_{x1}^1+f_{x1}^2)+\sum_{i=0}^{l-1}\beta_i f_{y1}+\sum_{i=0}^{l-1}\gamma_i f_{z1}=-p_x\\
&\sum_{i=0}^{l-1}\alpha_i f_{x2}+\sum_{i=0}^{l-1}\beta_i(f_{y2}^1+f_{y2}^2)+\sum_{i=0}^{l-1}\gamma_i f_{z2}=-p_y\\
&\sum_{i=0}^{l-1}\alpha_i f_{x3}+\sum_{i=0}^{l-1}\beta_i f_{y3}+\sum_{i=0}^{l-1}\gamma_i f_{z3}=-p_z
\end{aligned}\right\} \tag{5}$$

4. Numerical results and discussions

4.1 Definition of dimensionless stress intensity factors

On the basis of the theory described in section 3 computer programs are coded, and calculations are performed when the aspect ratio is a/b=1, 2, 4, 8, under Poisson ratio $\nu_1=\nu_2=0.3$ with varying polynomial exponents m,n. As a result, smooth distributions of stress intensity factor along the crack front are obtained. In demonstrating the numerical results of stress intensity factors (SIFs) K_I,K_{II},K_{III} , the following dimensionless factors F_I,F_{II},F_{III} will be used. Here, F_I,F_{II},F_{III} are expressed on the basis of the SIF ($\sigma_z^\infty\sqrt{\pi b}$) of 2D crack whose length is 2b.

$$F_I+iF_{II}=\frac{K_I(x,y)\big|_{x=x,y=\pm b}+iK_{II}(x,y)\big|_{x=x,y=\pm b}}{\tau_{yz}^\infty\sqrt{\pi b}}=\sqrt{a^2-x^2}\times(\cos\left(\varepsilon\ln(\frac{a-x}{a+x})\right)F_z(x,y)\big|_{x=x,y=\pm b}\,2i\varepsilon F_y(x,y)\big|_{x=x,y=\pm b})$$

$$F_{III}=\frac{K_{III}(x,y)\big|_{x=x,y=\pm b}}{\tau_{yz}^\infty\sqrt{\pi b}}=\sum_{l=1}^{2}\frac{1+\kappa_l}{4\mu_l\cosh\pi\varepsilon}\frac{1}{(1/G_1+1/G_2)}\times\sqrt{a^2-x^2}\sin\left(\varepsilon\ln(\frac{a-x}{a+x})\right)F_x\big|_{x=x,y=\pm b} \tag{6}$$

4.2 Compliance of boundary condition and convergence of numerical solutions

Table 1 shows the convergence of the results for F_{II},F_{III},F_I at $y=b$ when $\mu_1/\mu_2=2$, a/b=1, $\nu_1=\nu_2=0.3$ with varying polynomial exponents in Eq. (4). The boundary conditions are considered at the collocation point on the mesh 10×10 chosen the crack boundary. To minimize the residual stresses the coefficients $\alpha_i, \beta_i, \gamma_i$ in Eq. (5) are determined. From Table 3 it is seen that the results may be accurate until the 3-digit. Compliance of boundary conditions is shown in Fig.2 where the residual stresses, which should be zero along the crack surface, are less than 5.2×10^{-5} when $n=8$.

Table 1 Convergence of stress intensity factor at $y=b$ for $\mu_2/\mu_1=2$, a/b=1, $\nu_1=\nu_2=0.3$

	x/a	0/11	1/11	2/11	3/11	4/11	5/11	6/11	7/11	8/11	9/11	10/11
F_{II}	m=n=6	0.8419	0.8398	0.8336	0.8235	0.8098	0.7924	0.7702	0.7408	0.6981	0.6284	0.4966
	m=n=7	0.8419	0.8402	0.8349	0.8257	0.8120	0.7932	0.7688	0.7374	0.6956	0.6327	0.5131
	m=n=8	0.8428	0.8411	0.8359	0.8268	0.8132	0.7945	0.7695	0.7369	0.6936	0.6307	0.5154
F_I	m=n=6	0.0472	0.0471	0.0467	0.0460	0.0449	0.0433	0.0410	0.0380	0.0338	0.0283	0.0202
	m=n=7	0.0474	0.0472	0.0468	0.0461	0.0451	0.0436	0.0416	0.0388	0.0349	0.0295	0.0214
	m=n=8	0.0475	0.0473	0.0469	0.0461	0.0451	0.0437	0.0417	0.0391	0.0357	0.0312	0.0245
	y/b	0/11	1/11	2/11	3/11	4/11	5/11	6/11	7/11	8/11	9/11	10/11
F_{III}	m=n=6	0.6516	0.6500	0.6454	0.6376	0.6264	0.6111	0.5906	0.5624	0.5222	0.4607	0.3547
	m=n=7	0.6505	0.6490	0.6443	0.6364	0.6250	0.6098	0.5900	0.5638	0.5274	0.4717	0.3714
	m=n=8	0.6507	0.6490	0.6442	0.6360	0.6243	0.6088	0.5886	0.5626	0.5273	0.4743	0.3780

Table 2 Dimensionless stress intensity factor F_{II} and F_I for $a/b=8$ at $(0,b)$

μ_2/μ_1	2		5		10		100	
ν, ν	F_{II}	F_I ()	F_{II}	F_I	F_{II}	F_I ()	F_{II}	F_I ()
0,0	0.9930	0.1042(0.1072)	0.9834	0.2009(0.2206)	0.9742	0.2410(0.3298)	0.9373	0.2743(0.3476)
0,0.5	0.9768	0.2366(0.2698)	0.9671	0.2640(0.3122)	0.9626	0.2745(0.2766)	0.9576	0.2847(0.3414)
0.3,0.3	0.9975	0.0602(0.0608)	0.9952	0.1189(0.1228)	0.9933	0.1448(0.1516)	0.9905	0.1716(0.1832)

Table 3 Dimensionless stress intensity factor for a/b=1, ε =0.02 at $y=b$

	$\nu_1,\nu_2(\mu_2/\mu_1)$	x/a=0	1/11	2/11	3/11	4/11	5/11	6/11	7/11	8/11	9/11	10/11
F_{II}	0. 3, 0. 3	0.8419	0.8402	0.8350	0.8258	0.8123	0.7936	0.7687	0.7361	0.6928	0.6300	0.5149
	0,0(1.2870)	0.7544	0.7527	0.7475	0.7385	0.7253	0.7047	0.6837	0.6527	0.6112	0.5502	0.4412
	0,0.5(0.0718)	0.8982	0.8967	0.8917	0.8831	0.8700	0.8518	0.8275	0.7958	0.7548	0.6959	0.5825
F_I	0. 3, 0. 3	0.0313	0.0312	0.0309	0.0304	0.0297	0.0287	0.0275	0.0257	0.0235	0.0205	0.0161
	0,0(1.2870)	0.0278	0.0278	0.0275	0.0270	0.0263	0.0254	0.0241	0.0225	0.0203	0.0171	0.0121
	0,0.5(0.0718)	0.0337	0.0335	0.0332	0.0326	0.0320	0.0312	0.0299	0.0282	0.0262	0.0246	0.0235
	$\nu_1,\nu_2(\mu_2/\mu_1)$	y/b→0	1/11	2/11	3/11	4/11	5/11	6/11	7/11	8/11	9/11	10/11
F_{III}	0.3, 0.3(1.5628)	0.6529	0.6513	0.6464	0.6382	0.6265	0.6108	0.5906	0.5645	0.5291	0.4759	0.3796
	0,0(1.2870)	0.7518	0.7501	0.7449	0.7359	0.7229	0.7050	0.6814	0.6506	0.6092	0.5490	0.4415
	0,0.5(0.0718)	0.5741	0.5726	0.5682	0.5608	0.5505	0.5371	0.5202	0.4987	0.4694	0.4242	0.3395

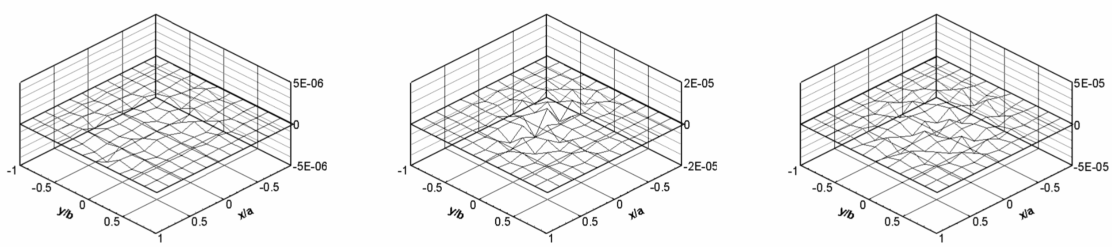

(a) $\frac{\sigma_z}{\tau_{yz}^{\infty}}$ (b) $\frac{\tau_{yz}}{\tau_{yz}^{\infty}}+1$ (c) $\frac{\tau_{zx}}{\tau_{yz}^{\infty}}$

Fig.2 Compliance of boundary condition when $\mu_2/\mu_1=2$, a/b=1, $\nu_1=\nu_2=0.3$

4.3 Comparison with the two-dimensional interface crack

When the aspect ratio of the crack a/b is very large and tends to infinity, the results should coincide with the two-dimensional solution. Table 2 shows the values of F_I, F_{II}, F_{III} when $m = n = 8$ with aspect ratio a/b=8. It is seen that the present results coincide with the two-dimensional exact solutions known as $F_{II} = 1, F_I = 2\varepsilon$ when $a/b \to \infty$ in the range of $|x/a| \le 0.5$.

4.4 The stress intensity factors under the same value of ε

In the preceding papers [12], [13], it is found that the stress intensity factors are controlled by bimaterial constant ε alone under tensile loading. In Table 3, Poisson's ratio and shear modulus ratio are changed under constant value of ε =0.02. As shown in Table 3, it is seen that the stress intensity factors are not controlled by ε alone under shear loading.

4.5 Effect of elastic modulus ratio μ_2/μ_1 on the stress intensity factors

For general aspect ratios, the following results are obtained by taking polynomial exponents $m = n$ =8 with the collocation points 10×10. The dimensionless stress intensity factors F_{II}, F_{III}, F_I are obtained with varying the elastic modulus ratio μ_2/μ_1 under ν_1=$\nu_2 = 0.3$ in Tables 4-7 and Fig.3. It is shown that the values of F_{II} and F_{III} are insensitive to the shear modulus ratios μ_2/μ_1. On the other hand, F_I values, which are positive at $x = a$ and negative at $x = -a$, are largely depending on μ_2/μ_1. Figure 4 shows distributions of stress intensity factors with varying a/b under $\mu_2/\mu_1 = 2$ and $\nu_1 = \nu_2 = 0.3$. As a/b increases, it is seen that the results coincide with the 2D exact solution $F_{II} = 1$, $F_I = 2\varepsilon$.

4.6 Effect of Poisson's ratio on the stress intensity factors

In Table 8, the dimensionless stress intensity factors F_{II}, F_{III}, F_I are indicated with varying Poisson's ratio under fixed values of μ_2/μ_1=2, a/b=1. It is seen that those values are varied depending on Poisson's ratio. When $\nu_1 = \nu_2 = 0$, F_{II} takes a minimum value, and F_{III} takes a maximum value of F_{III}. On the other hand, as $\nu_1 \to 0.5, \nu_2 \to 0.5$, F_{II} takes a maximum value, and F_{III} takes a minimum value. With increasing the value of ε, F_I value increases. Figure 5 shows distributions of stress intensity factors when $\mu_2/\mu_1 = 2$. The value of F_{II} and F_{III} are mainly controlled by Poisson's ratios, and the values of F_I is mainly controlled by ε.

Table4 Stress intensity factor at $y = b$ for a/b=1, $\nu_1 = \nu_2 = 0.3$

	G_2/G_1	x/a=0	1/11	2/11	3/11	4/11	5/11	6/11	7/11	8/11	9/11	10/11
F_{II}	2	0.8428	0.8411	0.8359	0.8268	0.8132	0.7945	0.7695	0.7369	0.6939	0.6307	0.5154
	5	0.8474	0.8457	0.8405	0.8214	0.8178	0.7990	0.7739	0.7411	0.6976	0.6345	0.5185
	10	0.8502	0.8486	0.8433	0.8342	0.8206	0.8018	0.7766	0.7438	0.7003	0.6371	0.5207
	100	0.8536	0.8519	0.8467	0.8376	0.8240	0.8051	0.7800	0.7472	0.7037	0.6404	0.5236
F_{III}	2	0.6507	0.6490	0.6442	0.6360	0.6243	0.6088	0.5886	0.5626	0.5273	0.4743	0.3780
	5	0.6388	0.6372	0.6324	0.6243	0.6129	0.5977	0.5781	0.5527	0.5181	0.4656	0.3696
	10	0.6307	0.6291	0.6243	0.6163	0.6050	0.5901	0.5708	0.5459	0.5118	0.4597	0.3638
	100	0.6200	0.6184	0.6137	0.6058	0.5947	0.5801	0.5613	0.5370	0.5035	0.4519	0.3563
F_I	2	0.0475	0.0473	0.0469	0.0461	0.0451	0.0437	0.0417	0.0391	0.0357	0.0312	0.0245
	5	0.0947	0.0944	0.0936	0.0921	0.0901	0.0873	0.0835	0.0785	0.0718	0.0631	0.0500
	10	0.1161	0.1157	0.1147	0.1129	0.1105	0.1071	0.1026	0.0965	0.0885	0.0781	0.0623
	100	0.1388	0.1384	0.1372	0.1351	0.1323	0.1284	0.1231	0.1160	0.1067	0.0945	0.0760

Table5 Stress intensity factor at $y = b$ for a/b=2 $\nu_1 = \nu_2 = 0.3$

	G_2 / G_1	0/11	1/11	2/11	3/11	4/11	5/11	6/11	7/11	8/11	9/11	10/11
F_{II}	2	0.9557	0.9546	0.9511	0.9448	0.9351	0.9209	0.9004	0.8714	0.8287	0.7600	0.6234
	5	0.9569	0.9558	0.9525	0.9463	0.9368	0.9228	0.9027	0.8739	0.8315	0.7630	0.6265
	10	0.9574	0.9563	0.9530	0.9470	0.9377	0.9238	0.9039	0.8753	0.8331	0.7648	0.6285
	100	0.9576	0.9566	0.9533	0.9474	0.9383	0.9247	0.9051	0.8768	0.8350	0.7670	0.6310
F_{III}	2	0.4707	0.4697	0.4668	0.4617	0.4542	0.4435	0.4286	0.4072	0.3759	0.3278	0.2473
	5	0.4604	0.4595	0.4567	0.4518	0.4446	0.4344	0.4199	0.3990	0.3682	0.3207	0.2412
	10	0.4535	0.4526	0.4499	0.4452	0.4382	0.4282	0.4140	0.3935	0.3631	0.3160	0.2370
	100	0.4444	0.4436	0.4410	0.4365	0.4297	0.4201	0.4063	0.3863	0.3564	0.3099	0.2316
F_I	2	0.0570	0.0569	0.0566	0.0560	0.0552	0.0541	0.0524	0.0499	0.0464	0.0409	0.0314
	5	0.1130	0.1128	0.1122	0.1113	0.1097	0.1075	0.1043	0.0996	0.0928	0.0822	0.0635
	10	0.1379	0.1376	0.1370	0.1359	0.1341	0.1314	0.1276	0.1221	0.1140	0.1012	0.0786
	100	0.1640	0.1638	0.1630	0.1617	0.1597	0.1567	0.1523	0.1460	0.1367	0.1219	0.0951

Table6 Stress intensity factor at $y = b$ for a/b=4 $\nu_1 = \nu_2 = 0.3$

	G_2 / G_1	0/11	1/11	2/11	3/11	4/11	5/11	6/11	7/11	8/11	9/11	10/11
F_{II}	2	0.9857	0.9855	0.9848	0.9834	0.9810	0.9766	0.9689	0.9556	09308	0.8788	0.7455
	5	0.9879	0.9877	0.9869	0.9854	0.9827	0.9780	0.9700	0.9560	0.9306	0.8008	0.7440
	10	0.9893	0.9890	0.9882	0.9866	0.9837	0.9788	0.9705	0.9561	0.9301	0.9768	0.7426
	100	0.9908	0.9905	0.9896	0.9878	0.9848	0.9795	0.9707	0.9557	0.9289	0.8748	0.7403
F_{III}	2	0.3402	0.3391	0.3360	0.3305	0.3224	0.3111	0.2959	0.2756	0.2485	0.2110	0.1550
	5	0.3328	0.3318	0.3287	0.3233	0.3152	0.3040	0.2890	0.2690	0.2423	0.2056	0.1506
	10	0.3279	0.3269	0.3238	0.3184	0.3104	0.2993	0.2844	0.2646	0.2381	0.2018	0.1476
	100	0.3215	0.3205	0.3174	0.3121	0.3042	0.2932	0.2784	0.2588	0.2327	0.1970	0.1436
F_I	2	0.0598	0.0597	0.0596	0.0595	0.0593	0.0589	0.0582	0.0569	0.0545	0.0503	0.0414
	5	0.1182	0.1182	0.1180	0.1178	0.1174	0.1168	0.1155	0.1131	0.1088	0.1007	0.0832
	10	0.1440	0.1439	0.1437	0.1435	0.1431	0.1424	0.1410	0.1383	0.1332	0.1236	0.1026
	100	0.1708	0.1707	0.1706	0.1703	0.1700	0.1693	0.1678	0.1649	0.1593	0.1483	0.1237

Table7 Stress intensity factor at $y = b$ for a/b=8 $\nu_1 = \nu_2 = 0.3$

	G_2 / G_1	0/11	1/11	2/11	3/11	4/11	5/11	6/11	7/11	8/11	9/11	10/11
F_{II}	2	0.9975	0.9975	0.9973	0.9970	0.9965	0.9954	0.9933	0.9895	0.9809	0.9533	0.8453
	5	0.9952	0.9951	0.9950	0.9947	0.9943	0.9933	0.9915	0.9880	0.9800	0.9535	0.8470
	10	0.9933	0.9933	0.9931	0.9929	0.9925	0.9916	0.9899	0.9867	0.9790	0.9533	0.8479
	100	0.9905	0.9904	0.9903	0.9901	0.9897	0.9890	0.9874	0.9845	0.9774	0.9527	0.8487
F_{III}	2	0.2248	0.2239	0.2212	0.2165	0.2099	0.2009	0.1893	0.1745	0.1556	0.1307	0.0949
	5	0.2185	0.2177	0.2150	0.2105	0.2039	0.1952	0.1839	0.1695	0.1511	0.1269	0.0921
	10	0.2143	0.2135	0.2108	0.2064	0.1999	0.1913	0.1802	0.1661	0.1481	0.1243	0.0901
	100	0.2090	0.2081	0.2055	0.2011	0.1948	0.1864	0.1755	0.1617	0.1441	0.1210	0.0876
F_I	2	0.0602	0.0602	0.0602	0.0602	0.0602	0.0601	0.0599	0.0597	0.0591	0.0569	0.0492
	5	0.1190	0.1190	0.1190	0.1190	0.1190	0.1189	0.1187	0.1184	0.1175	0.1136	0.0988
	10	0.1448	0.1448	0.1448	0.1448	0.1448	0.1448	0.1448	0.1445	0.1436	0.1392	0.1217
	100	0.1716	0.1716	0.1717	0.1719	0.1719	0.1720	0.1720	0.1720	0.1712	0.1666	0.1465

Table8 Stress intensity factor at $(0,b)$ for a/b=1, $\mu_2/\mu_1=2$

ν_1	ν_2	ε	F_{II}	F_{III}	F_I
0	0	0.0536	0.7603	0.7421	0.0740
0	0.1	0.0668	0.7725	0.7268	0.0930
0	0.2	0.0813	0.7855	0.7088	0.1138
0	0.3	0.0972	0.7992	0.6876	0.1365
0	0.4	0.1149	0.8134	0.6625	0.1614
0	0.5	0.1349	0.8276	0.6325	0.1887
0.1	0.1	0.0475	0.7858	0.7160	0.0682
0.1	0.2	0.0620	0.7983	0.6992	0.0896
0.1	0.3	0.0779	0.8117	0.6792	0.1133
0.1	0.4	0.0956	0.8258	0.6555	0.1392
0.1	0.5	0.1155	0.8401	0.6268	01679
0.2	0.2	0.0400	0.8132	0.6858	0.0598
0.2	0.3	0.0559	0.8260	0.6675	0.0843
0.2	0.4	0.0736	0.8397	0.6454	0.1114
0.2	0.5	0.0935	0.8540	0.6185	0.1416
0.3	0.3	0.0304	0.8428	0.6507	0.0475
0.3	0.4	0.0481	0.8557	0.6308	0.0757
0.3	0.5	0.0680	0.8696	0.6062	0.1075
0.4	0.4	0.0177	0.8749	0.6087	0.0389
0.4	0.5	0.0376	0.8878	0.5873	0.0621
0.4999	0.4999	→0	0.9098	0.5570	7x10^{-6}

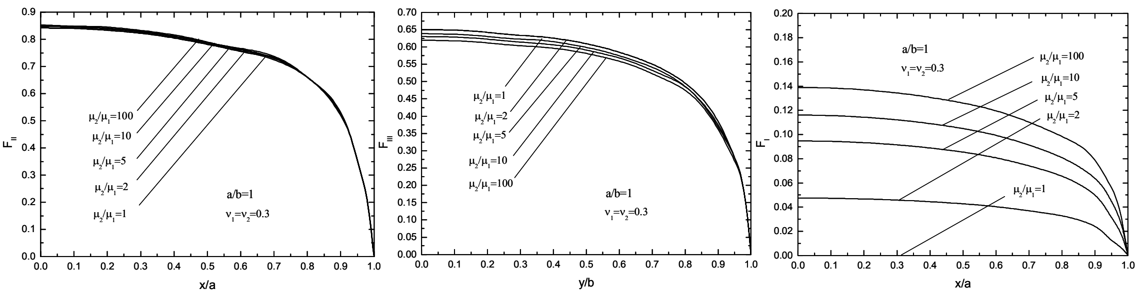

(a) F_{II} (b) F_{III} (c) F_I

Fig. 3 Variations of SIF for a/b=1, $\nu_1=\nu_2=0.3$

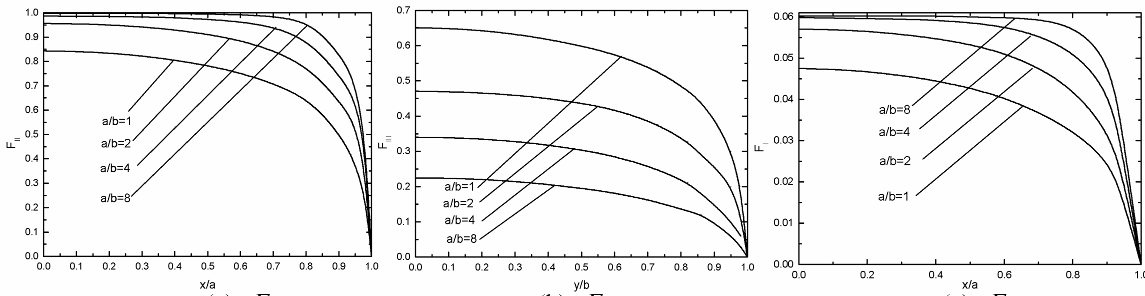

(a) F_{II} (b) F_{III} (c) F_I

Fig. 4 Variations of SIF for $\mu_2/\mu_1=2$, $\nu_1=\nu_2=0.3, 2\varepsilon=0.0608$

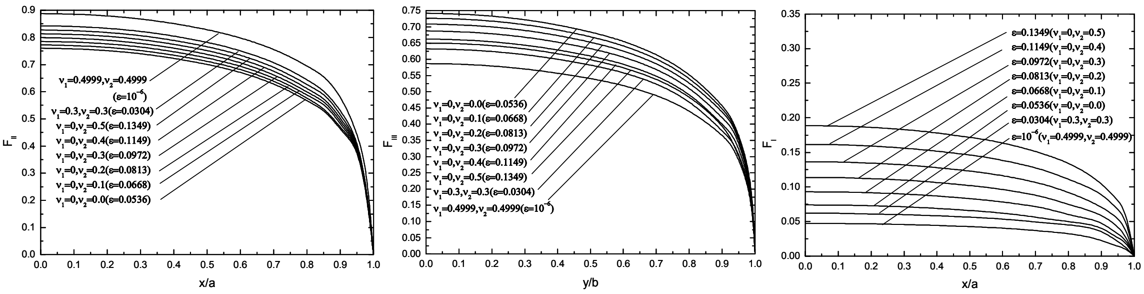

(a) F_{II} (b) F_{III} (c) F_I

Fig. 5 Variations of SIF for a/b=1, $\mu_2/\mu_1=2$

5. Conclusion

In the present paper, a planar rectangular interfacial crack in a three-dimensional bimaterial under shear loading is considered by means of the singular integral equations based on the body force method. The conclusion can be made in the following way.

(1) The unknown functions are approximated by using the fundamental density functions and polynomials. It is found that the present method shows good convergence of the results and boundary conditions are satisfied very accurately (see Table 2 and Fig. 2). The results for a/b=8 coincide with the exact solutions of 2D interfacial crack.

(2) The dimensionless stress intensity factors F_{II}, F_{III} are insensitive to the elastic modulus ratio μ_2/μ_1. Those values are mainly determined from the aspect ratio of the crack a/b and Poisson's ratios of the materials ν_1, ν_2

(3) Under the constant value of elastic modulus ratio μ_2/μ_1, the F_I value increases with increasing the value of ε. On the other hand, the value of F_{II} and F_{III} are mainly controlled by Poisson's ratios (see Tables 4-7, Figs.3-5)...

References

(1) Mossakovski, V. I., and Rybka, M. T., Generalization of the Griffith-Sneddon Criterion for the Case of a Non-homogeneous Body, Prikladnaia metematica I mekhanika. Vol. 28, (1964), pp.1061-1069

(2) England, F., Stress Distribution in Bonded Dissimilar Materials Containing Circular or Ring-Shaped Cavities, *Transaction of the ASME, Journal of Applied Mechanics, Series E*, Vol. 32, (1965), pp.829-836

(3) Kassir, M.K., and Bregman, A. M., The Stress Intensity Factor for a Penny-Shaped Crack between Two Dissimilar Materials, *Transaction of the ASME, Journal of Applied Mechanics, Series E*, Vol. 39, (1972), pp.308-310

(4) Lowengrub, M. and Sneddon,I. N., The Effect of Internal Pressure on a Penny-Shaped Crack at the Interface of Two Bonded Dissimilar Elastic Half-Spaces, *International Journal of Engineering Science*, Vol. 12, (1974), pp.387-396

(5) Keer, L. M. Chen, S. H. and Comninou,M., The Interface Penny-Shaped Crack Reconsidered, *International Journal of Engineering Science*, Vol.16, (1978), pp. 765-772

(6) Shibuya, T., Koizumi, T., Iwamoto, T., Stress Analysis of the Vicinity of an Elliptical Crack at the Interface of Two Bonded Half-Spaces, *JSME International Journal, Series A,* Vol.32, (1989), pp.485-491

(7) Yuuki, R., Cao, X. F., Boundary Element Analysis to Stress Intensity Factor of Interface Crack, *Transaction of the Japan Society of Mechanical Engineering, Series A,* (in Japanese) No.55-510,(1989), pp.340-347

(8) Takakuda, K., Shibuya, T., and Koizumi, T., Stress Analysis for biomaterial with an Interface Crack, *In: Prelim. Proc. 55th Annual Meeting of Japan Soc. Mech. Engrs.,* (in Japanese) No. 780-3, (1978), pp.167-169

(9) Noda, N.A., Kagita, M., and Chen, M,C., Analysis of Stress Intensity Factors of a Ring-Shaped Interface Crack, *International Journal of Solids and Structures*, Vol.40, No.24, (2003), pp.6577-6592

(10) Qing W. and Noda, N.A.,Variation of Stress Intensity Factors along the Front of 3D Rectangular Crack by Using a Singular Integral Equation Method, *International Journal of Fracture*, Vol. 108,(2001), pp.119-131

(11) Qin T.Y. and Noda, N. A., Stress Intensity Factors of Rectangular Crack Meeting a Bimateral Interface, *International Journal of Solids and Structures,* Vol. 40,(2003),

pp.2473-2486

(12) Noda, N.A., Xu, C. H., and Takase, Y., Stress Intensity Factor for a Planar Interfacial Crack in Three Dimensional Bimaterials, *Transaction of the Japan Society of Mechanical Engineering, Series A* (in Japanese, submitted)

(13) Noda, N.A., Xu, C. H., and Takase, Y., Stress Intensity Factor for a rectangular Interface Crack in Three Dimensional Bimaterials, *Transaction of the Japan Society of Mechanical Engineering, Series A* (in Japanese, submitted)

(14) Chen M. C. Noda, N. A. and Tang, R. J.,, Application of Finite-part Integrals to Planar Interfacial Fracture Problems in Three Dimensional Bimaterials, *Journal of Applied Mechanics*, Vol.66, (1999), pp.885-890